ISSN 1070-3284, Russian Journal of Coordination Chemistry, 2018, Vol. 44, No. 1, pp. 72–81. © Pleiades Publishing, Ltd., 2018.

Syntheses, Crystal Structures, and Properties of Two d^{10} Metal Complexes Based on Ferrocenyl Ligands Bearing Pyrazolyl Pyridine Substituents[1]

W. Liu[a], X. Li[a, *], H. H. Chen[a], B. L. Wu[b, **], and H. Y. Zhang[b]

[a]*College of Materials and Chemical Engineering, Henan University of Urban Construction, Pingdingshan, Henan, 467044 P.R. China*

[b]*College of Chemistry and Molecular Engineering, Zhengzhou University, Zhengzhou, Henan, 450052 P.R. China*

**e-mail: lixia@hncj.edu.cn*

***e-mail: wbl@zzu.edu.cn*

Received March 21, 2017

Abstract—Two new complexes, namely, $[Cd_2(L^1)_2(NCS)_4(DMF)_2] \cdot 4H_2O$ (**I**) and $\{[Zn_3(L^2)_4(SO_4)_3(H_2O)_8] \cdot 3DMF \cdot 6H_2O\}_n$ (**II**) have been synthesized through self-assembly of Cd(II) or Zn(II) salts with ferrocenyl ligands bearing pyrazolyl pyridine substituents. The two compounds were characterized by IR spectra, element analysis, X-ray powder diffraction, single-crystal X-ray diffraction (CIF files CCDC nos. 949526 (**I**), 949527 (**II**)), and thermogravimetric analysis. Complex **I** crystallizes in the monocline space group $P2_1/c$ and exhibits a discrete dinuclear structure. The adjacent dinuclear molecules are packed into a 1D linear chain through the hydrogen-bond interactions. Complex **II** is a neutral one-dimensional infinite zigzag coordination chain. The 3D packing diagram of **II** contains two types of voids and the solvated DMF and water molecules filled them and stabilized by the hydrogen bonds. In addition, the redox properties of both complexes **I** and **II** have also been investigated.

Keywords: ferrocenyl ligands bearing pyrazolyl pyridine substituents, Cd(II) complex, Zn(II) complex, redox property

DOI: 10.1134/S1070328417120053

INTRODUCTION

The design and construction of novel metal-organic frameworks (MOFs) have attracted considerable attention over the past few decades, not only for their diverse structural topologies but also for their potential application in the areas of magnetism, luminescence, gas storage, ion-exchange and optical properties, etc. [1–6]. Up to now, considerable progress in MOFs has been made; however, rational prediction and controllable synthesis of MOFs are still a great challenge for chemists, mainly due to the complexity of the factors influencing the self-assembly progress, including the nature of ligands, coordination geometry of the metal ions, counter-anions, pH values, solvents, temperatures and so forth. From the view of crystal engineering, the most effective strategy to construct anticipative structure is to employ appropriate organic linker which can bind metal centers through direct bond formation. The bipyridyl based N-heterocyclic ligands [7–15] have proven to be excellent ligands for building novel coordination frameworks. By incorporating different bridging groups (such as amide-benzene-bridging group, carbonylpiperazine-bridging group, amide-$(CH_2)_n$-bridging group) into bipyridyl backbone, numerous derivatives of bipyridyl are obtained. For example, Wang's group has reported a novel 3-fold interpenetrating three-dimensional metal-organic framework $[Cu_3(4\text{-Bpcb})_3(BTC)_2]_{3n}$ with (3,4)-connected $(6^3)(6^4 10^2)$ topology (4-Bpcb = *N*,*N*'-bis(4-pyridinecarboxamide)-1,4-benzene, H_3BTC = 1,3,5-benzenetricarboxylic acid), in which discrete cagelike $(H_2O)_{12}$ water cluster guests occupy the voids [8]. LaDuca's group has reported a series of 2D and 3D polymers based on the bis(4-pyridylformyl)piperazine ligand and aromatic dicarboxylate ligands [10, 11].

On the other hand, owing to their special chemical and electrochemical properties, ferrocene and its derivates have been extensively studied and increasingly become an active research area. In the field of coordination chemistry, the ferrocene molecule has been widely used as a building block for polynuclear complexes, polymers, supramolecular aggregates, and many other species exhibiting a wide range of proper-

[1] The article is published in the original.

ties [16]. As the literature reported, two types of ferrocenyl derivatives have been widely used as ligands: ferrocenyl-based carboxylate [17–21] and pyridine-containing ferrocene [22–26]. We are interested in designing more ferrocenyl ligands to obtain more desired complexes, and in our previous work we incorporated the isophenyiacid unit into ferrocene and tested the coordination capabilities of the resulting ligand toward transition metal salts [18]. Very recently, we attempted to introduce the ferrocene group into the bipyridyl-based organic ligands and obtain the ligands 1,1'-[bis-3-(4-pyridyl)pyrazol-5-yl]ferrocene (L^1) and 1,1'-[bis-3-(3-pyridyl)pyrazol-5-yl]ferrocene (L^2). We have used L^2 to assemble with $Cd(CH_3COO)_2$ in a CH_3OH–DMF solution and obtained a chiral 1D left-handed helical chain [27], while the metal complexes based on L^1 have never been reported. As a continuous work, we have selected other metal salts to reaction with L^1 and L^2 and obtained two new complexes, namely, $[Cd_2(L^1)_2(NCS)_4(DMF)_2] \cdot 4H_2O$ (**I**) and $\{[Zn_3(L^2)_4(SO_4)_3(H_2O)_8] \cdot 3DMF \cdot 6H_2O\}_n$ (**II**). Here we want to report their preparations, crystal structures and redox properties.

EXPERIMENTAL

Materials and general methods. All chemical reagents were obtained from commercial sources and solvents were purified by standard method. IR spectra were recorded on a Bruker VECTOR22 spectrophotometer with KBr pellets in 400–4000 cm^{-1} region. Elemental analyses (C, H, N, and S) were carried out on a Flash EA 1112 elemental analyzer. Thermal analysis curves were scanned in a range of 30–800°C with air atmosphere on STA 409 PC thermal analyzer. Cyclic voltammograms studies were recorded with a RST5000 electrochemical system (Zhengzhou Shiruisi Instrument Co. Ltd., Zhengzhou, China) utilizing the three-electrode configuration of a GC working electrode, a Pt auxiliary electrode, and a saturated calomel electrode as the reference electrode. The measurements were performed in DMF solution containing tetrabutyl ammonium perchlorate (TBAP, 0.1 M) as the supporting electrolyte. The potential was scanned from 0.0 to 1.0 V. Powered X-ray diffraction (PXRD) patterns of the samples were recorded by a RIGAKU-DMAX2500 X-ray diffractometer with CuK_α radiation.

General synthesis of ligands L^1 and L^2 (Scheme 1). 0.81 g (3.0 mmol) 1,1'-diacetylferrocene were dissolved in 20 mL abs. THF and treated with 0.48 g (12.0 mmol) NaH (60% in mineral oil) at room temperature. After 1 h of stirring 1.64 g (12.0 mmol) methyl isonicotinate (or methyl nicotinate) were added. Then the reaction mixture was refluxed for 4 h, cooled down to room temperature, and the forming red precipitate was collected by filtration. A mixture of the resulting red precipitate and 80% hydrazine hydrate (4.0 mL) was refluxed in ethanol (30 mL) with AcOH (1.0 mL) as catalysis for 2 h. The mixture then was cooled to room temperature and filtrated to give corresponding ligands as orange microcrystalline solid.

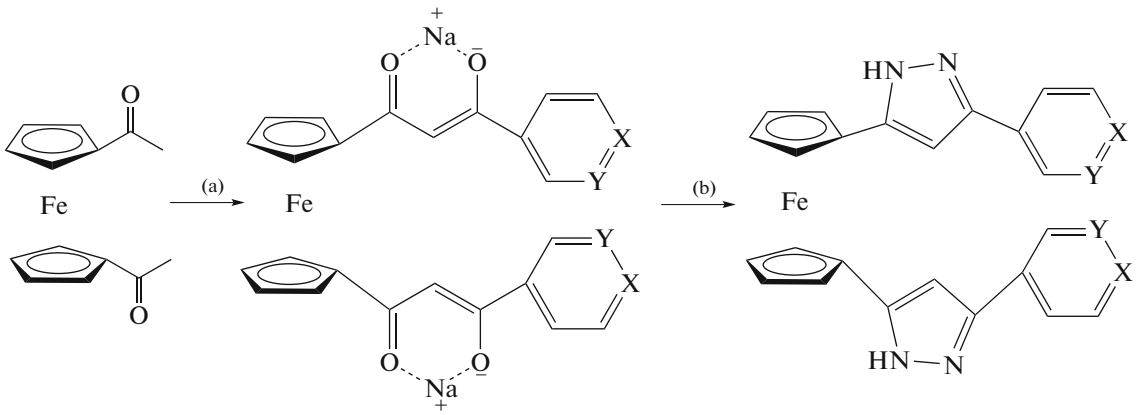

(a) NaH, methyl isonicotinate (or methyl nicotinate)—THF,
(b) $NH_2NH_2 \cdot H_2O$, AcOH–MeOH, refluxing.

Scheme 1.

The crude product was recrystallized from DMF–MeOH. The yields of ligands L^1 and L^2 are 37.2 and 38.4%, respectively.

For $C_{26}H_{20}FeN_6$ (L^1)

anal. calcd., %	C, 66.12	H, 4.27	N, 17.79
Found, %	C, 66.26	H, 4.15	N, 17.72

IR (KBr; ν, cm^{-1}): 3421 w, 3133 m, 3033 m, 2911 m, 2862 m, 1606 s, 1446 m, 1219 w, 1180 w, 1030 m, 871 m, 825 m, 694 m, 520 m.

For $C_{26}H_{20}FeN_6$ (L^2)

anal. calcd., %	C, 66.12	H, 4.27	N, 17.79
Found, %	C, 66.23	H, 4.19	N, 17.82

IR (KBr; ν, cm^{-1}): 3126 s, 3028 s, 2907 s, 2863 s, 1600 m, 1569 m, 1460 m, 1438 m, 1414 s, 1284 m, 1178 m, 1030 s, 977 m, 960 m, 876 m, 815 s, 785 s, 704 s, 624 w, 519 m.

Synthesis of I. At room temperature, a methanol solution (5 mL) of $Cd(NO_3)_2 \cdot 4H_2O$ (0.0308 g, 0.1 mmol) was added dropwise to an DMF solution (10 mL) of L^1 (0.0472 g, 0.1 mmol) with continuous stirring for 10 min, and then a water solution (5 mL) of KSCN (0.0194 g, 0.2 mmol) was added dropwise into the above mixture to give a clear solution. The resulting orange solution was allowed to slowly evaporate at ambient temperature in the dark. One month later, dark red block crystals suitable for X-ray single crystal diffraction analysis were obtained in 56% yield based on Cd.

For $C_{31}H_{31}N_9O_3S_2FeCd$

anal. calcd., %	C, 45.97	H, 3.86	N, 15.56	S, 7.92
Found, %	C, 46.25	H, 3.96	N, 15.66	S, 8.06

IR (KBr; ν, cm^{-1}): 3170 s, 2921 s, 2072 s, 1993 m, 1655 s, 1612 s, 1448 m, 1391 m, 1220 m, 1182 w, 1114 m, 967 m, 832 m, 793 m, 705 m, 521 m.

Synthesis of II. At room temperature, a water solution (5 mL) of $ZnSO_4 \cdot 7H_2O$ (0.0288 g, 0.1 mmol) was added dropwise to an DMF solution (10 mL) of L^2 (0.0472 g, 0.1 mmol) with continuous stirring for ten minutes. The resulting orange solution was allowed to slowly evaporate at ambient temperature in the dark. Three weeks later, dark red block crystals suitable for X-ray single crystal diffraction analysis were obtained in 48% yield based on Zn.

For $C_{104}H_{80}N_{24}O_{20}S_3Fe_4Zn_3$

anal. calcd., %	C, 49.93	H, 3.22	N, 13.44	S, 3.85
Found, %	C, 47.29	H, 3.36	N, 12.52	S, 3.67

IR (KBr; ν, cm^{-1}): 3227 s, 2919 m, 1686 m, 1656 m, 1620 m, 1441 m, 1424 m, 1110 v.s, 1034 s, 964 m, 814 m, 793 m, 703 m, 620 m, 509 w.

X-ray structure determination. Crystallographic data for tαhe title compound was collected at 173(2) K on a Bruker SMART APEX-II CCD diffractometer equipped with a graphite crystal and incident beam monochromator using MoK_α radiation (λ = 0.71073 Å). Absorption corrections were applied by using SADABS. The structures were solved by direct methods and expanded with Fourier techniques. All of the non-hydrogen atoms were refined anisotropically. The hydrogen atoms were assigned with common isotropic displacement factors and included in the final refinement by using geometrical restrains. All calculations were performed using the SHELXL-97 crystallographic software package [28, 29]. Crystallographic crystal data and processing parameters are summarized in detail in Table 1. Selected bond lengths and bond angles are listed in Table 2. Hydrogen bonds of complex **I** are listed in Table 3.

Supplementary material for structures has been deposited with the Cambridge Crystallographic Data Centre (CCDC nos. 949526 (**I**), 949527 (**II**); deposit@ccdc.cam.ac.uk or http://www.ccdc.cam.ac.uk).

RESULTS AND DISCUSSION

Complex **I** exhibits a discrete dinuclear structure as shown in Fig. 1. The asymmetric unit of **I** contains one Cd^{2+} ion, one ligand L^1, two SCN^- anions, one coordinated DMF and two solvated water molecules. The center Cd^{2+} ion is six-coordinated, showing a slightly distorted octahedral geometry coordination environment. The equatorial plane is defined by three nitrogen atoms from three NCS^- anions and one oxygen atom from a DMF molecule. The Cd atom is located at 0.2207(2) Å above the equatorial plane. The axial positions are occupied by two pyridyl nitrogen (N(3) and N(6)) atoms from two different L^1 ligands. The bond angle of N(3)Cd(1)N(6) is 176.14(7)°. The Cd–N bond distances are in the range of 2.275(3)–2.457(2) Å, while the Cd–O bond distances are 2.326(2) Å. The Cd–O and Cd–N bond distances are all in the normal range [27, 30].

Within the ferrocene fragments, the Fe–C bond distances are in the range of 2.022(3)–2.054(3) Å. The planar cyclopentadienyl (Cp) rings of the ferrocenyl unit are nearly parallel to each other (the interplanar distance (angle) is 3.928 Å (123°)). The Cp rings are essentially eclipsed and the Fe-centroid distances are 1.6402(6) Å (Cg1) and 1.6424(6) Å (Cg2) with Cg1 and Cg2 are the centroids of the C(1)–C(5) and C(6)–C(10) rings. The Cg1Fe(1)Cg2 angle is 177.26(4)°. In compound **I**, although the ligands are 1,1'-disubstituted, the two arms of the ligand are not equal due to the steric hindrance, where the dihedral

Table 1. Crystallographic data and structure refinements for complexes **I**, **II**

Parameter	Value	
	I	**II**
Formula weight	810.02	2841.09
Crystal system	Monoclinic	Orthorhombic
Space group	$P2_1/c$	$Cmc2_1$
Unit cell dimensions:		
a, Å	15.934(7)	
b, Å	9.579(4)	62.638(8) Å
c, Å	22.146(10)	19.398(3) Å
β, deg	97.216(5)	9.8176(13) Å
Volume, Å^3	3353(3)	11929(3)
Z	4	4
ρ_{calcd}, mg/m^3	1.604	1.582
Absorptin coefficient, mm^{-1}	1.239	1.207
F(000)	1640	5864
Crystal size, mm	0.397 × 0.300 × 0.110	0.408 × 0.242 × 0.145
θ Range for data collection, deg	2.32–28.29	2.47–25.00
Index ranges	$-21 \le h \le 21$, $-12 \le k \le 12$, $-29 \le l \le 29$	$-71 \le h \le 74$, $-23 \le k \le 23$, $-11 \le l \le 11$
Reflections collected	29612	33907
Independent reflections (R_{int})	8264 (0.0329)	10508 (0.0379)
Refinement method	Full-matrix least-squares on F^2	Full-matrix least-squares on F^2
Data/restraints/parameters	8264/4/441	10508/1/830
Goodness-of-fit on F^2	1.016	1.026
Final R indices ($I > 2\sigma(I)$)	$R_1 = 0.0336$, $wR_2 = 0.0771$*	$R_1 = 0.0399$, $wR_2 = 0.0967$
R indices (all data)	$R_1 = 0.0508$, $wR_2 = 0.0858$*	$R_1 = 0.0527$, $wR_2 = 0.1048$
Largest diff. peak and hole, e Å^{-3}	0.439 and –0.472	0.499 and –0.310

* $R_1 = \Sigma\|F_o| - |F_c\|/\Sigma|F_o|$; $wR_2 = [\Sigma(F_o^2 - F_c^2)^2/\Sigma w(F_o^2)^2]^{1/2}$.

angle between pyrazole ring and pyridine ring in one arm is 19.71(8)°, while the other is 22.07(8)°.

In **I**, there are two coordinated types of NCS^- anions. One is terminal, while the other bridges two Cd(II) ions in an end-on fashion. The bridging NCS ligands are perpendicular to Cd–Cd axis with CdNCd angle of 98.39(8)°. Both bridging and terminal NCS ligands are almost linear with the bond angles of NCS being 177.17(27)° and 179.12(28)°, respectively. Each L^1 ligand serves as a bisconnector through its two pyridyl moieties producing a dinuclear metal ring, and the distance of two Cd^{2+} ions in the metal ring is 3.6660(11) Å. Moreover, the adjacent dinuclear molecules are packed into a 1D chain through the N–H···O and O–H···N hydrogen-bond interactions (Table 3), originating from the pyrazol hydrogen atoms and solvated water hydrogen atoms, respectively, to the solvated water oxygen atoms and the pyrazol nitrogen atoms (Fig. 2).

Single-crystal X-ray diffraction analyses reveal that complex **II** is a neutral one-dimensional infinite zigzag coordination chain. The asymmetric unit of **II** contains one and half crystallographically unique Zn(II) centers, two independent L^2 ligands, one and half SO_4^{2-} anions, four coordinated water molecules, one and half lattice DMF molecules and three lattice water molecules. As shown in Fig. 3, the Zn(1) center is six-coordinate and surrounded by two nitrogen atoms from two individual L^2 ligands, four oxygen atoms from one SO_4^{2-} anion and three coordinated water molecules, showing a distorted $[ZnO_4N_2]$ octahedral coordination geometry. The Zn(2) center is also six-coordinate and surrounded by two nitrogen atoms from two individual L^2 ligands, four oxygen

Table 2. Selected bond lengths (Å) and angles (deg) for complex **I** and **II***

Bond	*d*, Å	Bond	*d*, Å
		I	
Cd(1)–N(8)	2.275(3)	Cd(1)–N(6*A*)	2.314(2)
Cd(1)–N(3)	2.323(2)	Cd(1)–O(1)	2.326(2)
Cd(1)–N(7)	2.386(2)	Cd(1)–N(7*A*)	2.457(2)
		II	
Zn(1)–O(4)	2.054(4)	Zn(1)–O(8)	2.089(4)
Zn(1)–N(1)	2.094(4)	Zn(1)–O(9)	2.117(3)
Zn(1)–N(2)	2.134(4)	Zn(1)–O(10)	2.382(5)
Zn(2)–O(1)	2.118(5)	Zn(2)–N(3)	2.116(3)
Zn(2)–N(3*A*)	2.116(3)	Zn(2)–O(2)	2.150(4)
Zn(2)–O(11)	2.139(4)	Zn(2)–O(3*B*)	2.217(4)
Angle	ω, deg	Angle	ω, deg
		I	
N(8)Cd(1)N(6*A*)	89.72(9)	N(8)Cd(1)N(3)	88.57(9)
N(6*A*)Cd(1)N(3)	176.14(7)	N(8)Cd(1)O(1)	96.97(10)
N(6A)Cd(1)O(1)	86.30(7)	N(3)Cd(1)O(1)	97.35(7)
N(8)Cd(1)N(7)	100.04(10)	N(6*A*)Cd(1)N(7)	89.81(8)
N(3)Cd(1)N(7)	87.08(8)	O(1)Cd(1)N(7)	162.53(8)
N(8)Cd(1)N(7*A*)	177.49(9)	N(6*A*)Cd(1)N(7*A*)	92.19(8)
N(3)Cd(1)N(7*A*)	89.62(8)	O(1)Cd(1)N(7*A*)	81.54(8)
N(7)Cd(1)N(7*A*)	81.60(8)		
		II	
O(4)Zn(1)O(8)	162.85(18)	O(4)Zn(1)N(1)	87.14(16)
O(8)Zn(1)N(1)	90.35(16)	O(4)Zn(1)O(9)	90.73(15)
O(8)Zn(1)O(9)	89.62(15)	N(1)Zn(1)O(9)	172.64(15)
O(4)Zn(1)N(2)	98.65(19)	O(8)Zn(1)N(2)	98.50(14)
N(1)Zn(1)N(2)	98.22(15)	O(9)Zn(1)N(2)	89.07(14)
O(4)Zn(1)O(10)	83.4(2)	O(8)Zn(1)O(10)	79.60(17)
N(1)Zn(1)O(10)	88.26(17)	O(9)Zn(1)O(10)	84.49(16)
N(2)Zn(1)O(10)	173.28(17)	N(3*A*)Zn(2)N(3)	171.70(19)
N(3*A*)Zn(2)O(1)	93.28(10)	N(3)Zn(2)O(1)	93.28(10)
N(3*A*)Zn(2)O(11)	87.50(8)	N(3)Zn(2)O(11)	87.50(8)
O(1)Zn(2)O(11)	89.30(18)	N(3*A*)Zn(2)O(2)	92.86(9)
N(3)Zn(2)O(2)	92.86(9)	O(1)Zn(2)O(2)	84.20(18)
O(11)Zn(2)O(2)	173.49(19)	N(3*A*)Zn(2)O(3*B*)	87.02(10)
N(3)Zn(2)O(3*B*)	87.01(10)	O(1)Zn(2)O(3*B*)	173.85(17)
O(11)Zn(2)O(3*B*)	96.85(17)	O(2)Zn(2)O(3*B*)	89.65(17)

* Symmetry transformations used to generate equivalent atoms: (*A*) $-x + 1, -y, -z$ (**I**); (*A*) $-x, y, z$; (*B*) $-x, -y, z + 1/2$ (**II**).

atoms from two SO_4^{2-} anion and two coordinated water molecules, also giving a distorted $[ZnO_4N_2]$ octahedral coordination geometry. The Zn–O bond distances are in the range of 2.054(4)–2.382(5) Å, while the Zn–N bond distances are in the range of 2.094(4)–2.134(4) Å. Those parameters can be compared with those of the six-coordinated Zn^{2+} ion with octahedral coordination geometry in literature reported complexes [31, 32].

In **II**, the L^2 ligands exhibit two coordination modes: one links two Zn^{2+} ions using its two pyridyl groups, while the other only coordinated to one Zn^{2+}

Table 3. Geometrui parameters of hydrogen bonds for complex **I***

D–H···A	Distance, Å			Angle D–H···A, deg
	D–H	H···A	D···H	
		I		
O(2)–H(1*w*)···N(5*B*)	0.85	2.02	2.874(3)	176
O(3)–H(3*w*)···N(2*B*)	0.86	1.98	2.791(4)	158
N(1)–H(1)···O(2)	0.88	2.01	2.872(3)	168
N(4)–H(4)···O(3)	0.82	1.94	2.755(4)	173

* Symmetry transformations used to generate equivalent atoms: (*B*) $-x, -y-1, -z$.

ion using its one pyridyl group and the other being free. Owing to the different coordination modes, the dihedral angle between pyrazole ring and pyridine ring in two unique ligands are obviously different: the bis-connected one with the dihedral angles being 19.35(20)° and 27.69(20)°, while the other being 3.10(23)° and 8.70(22)°, respectively. Moreover, there are two coordinated types of SO_4^{2-} anions. One is terminal and the other bridges two Zn(II) ions forming a 1D zigzag chain in which the unit of $Zn(L^2)_2(SO_4^{2-})(H_2O)_3$ symmetrically hang on the two sides of the main chain (Fig. 4). Finally, a 3D supramolecular framework of **II** forms through the π···π interactions between the pyridyl ring and Cp ring and the C–H···π interactions originating from the C(8)–H(8) in the Cp ring to the pyrazolyl ring in adjacent chains. As shown in Fig. 5, each 1D zigzag chain is surrounded by other six 1D zigzag chains, and the 3D supermolecular contains two types of voids which are occupied by the solvated water molecules and stabilized by the hydrogen bonds.

To confirm whether the analyzed crystal structures are truly representative of the bulk materials, powder X-ray diffraction experiments were carried out for complexes **I** and **II**. The main peaks in the experimental spectra of **I** and **II** are well consistent with simulated ones, indicating the phase purity of those synthesized crystalline products. The differences in intensity may be due to the preferred orientation of the powder samples.

Thermogravimetric (TG) a alysis of complexes **I** and **II** were carried out at a heating rate of 10°C min^{-1} under air atmosphere. The TG curve (Fig. 6) revealed that **I** exhibits an initial weight loss starting at about 55°C with the observed weight loss of 3.82% corresponding to the release of the lattice water molecules (calcd. 4.44%). The second weight loss of 10.38% occurred between 146–200°C, which is attributed to the release of the coordination DMF molecules (calcd. 9.02%). An abrupt drop in TG curve occurs in

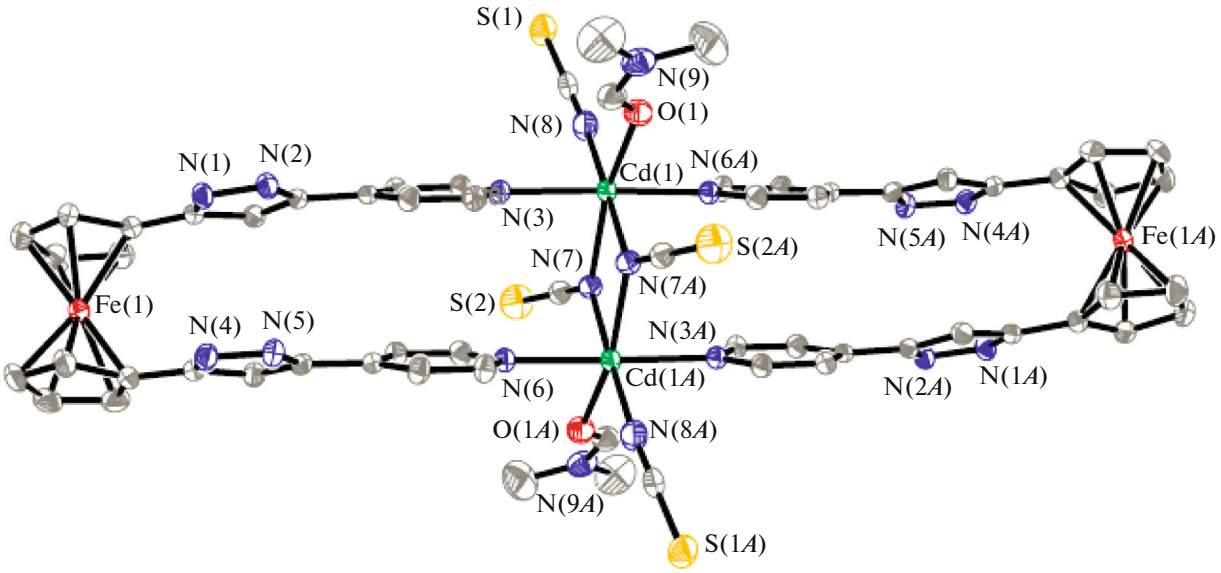

Fig. 1. Perspective view of the coordination environment of the Cd^{2+} ion in **I** (hydrogen atoms and guest molecules H_2O are omitted for clarity).

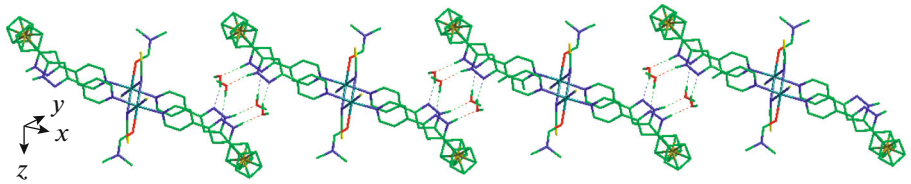

Fig. 2. The 1D linear chain bridged by the hydrogen bonding in complex **I**. The hydrogen bonding interactions between the chains are indicated as dotted line.

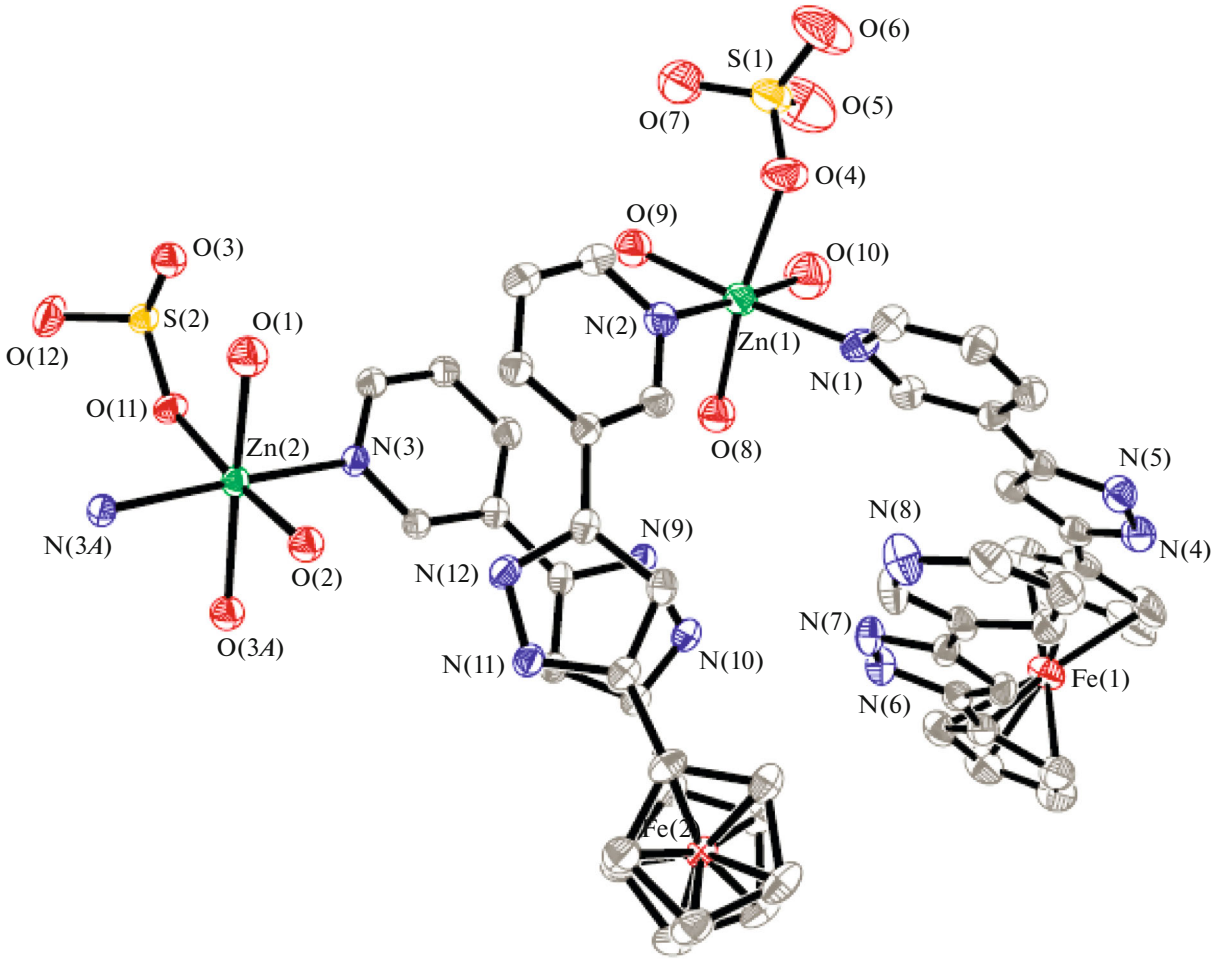

Fig. 3. Perspective view of the coordination environment of the Zn^{2+} ion in **II** (hydrogen atoms and guest molecules H_2O and DMF are omitted for clarity).

a temperature range of 302–437°C, which may indicate the decomposition of base frameworks. For **II**, the first weight loss of 11.24% occurred in the temperature range of 60–180°C, probably corresponding to the remove of all coordinated and crystallization solvent water and DMF molecules (calcd. 16.58%). The deviations may be due to the easy loss of lattice solvent molecules under ambient temperature. On further heating, the base framework of **II** began to decompose rapidly. The left residue of 22.90% can be attributed to the formation of ZnO, Fe_2O_3 (calcd. 19.85%) and deposition carbon.

The electrochemical behaviors of complexes **I**, **II** and free ligands L^1, L^2 were studied by cyclic voltammograms in DMF (Table 4 and Fig. 7). Compared with unsubstituted ferrocene, the half-wave potentials

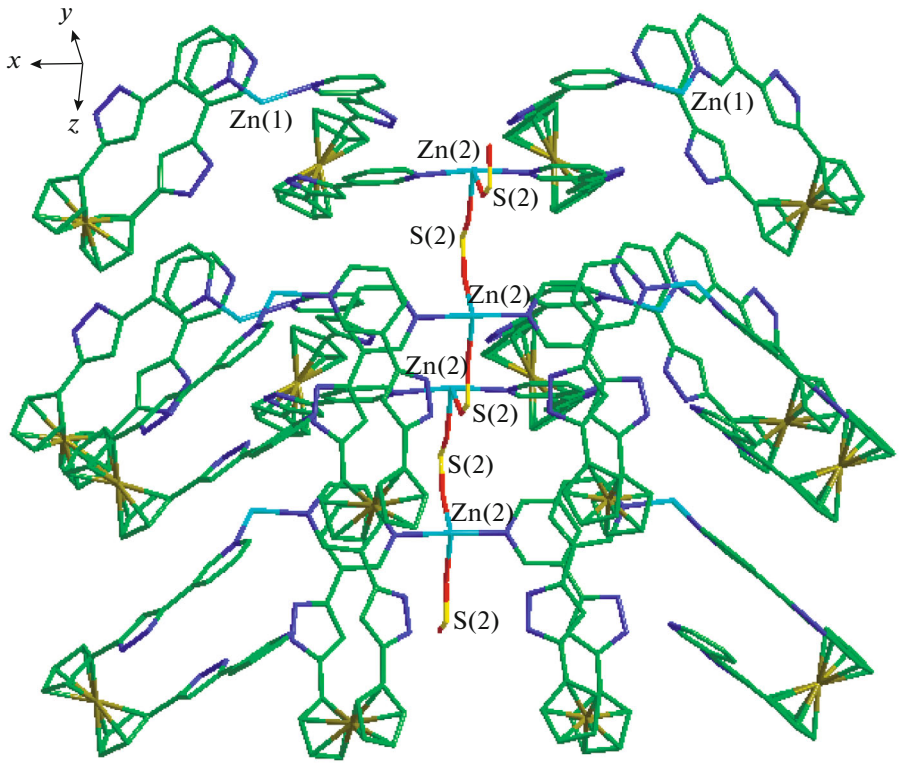

Fig. 4. The 1D zigzag chain bridged by the SO_4^{2-} in complex **II**.

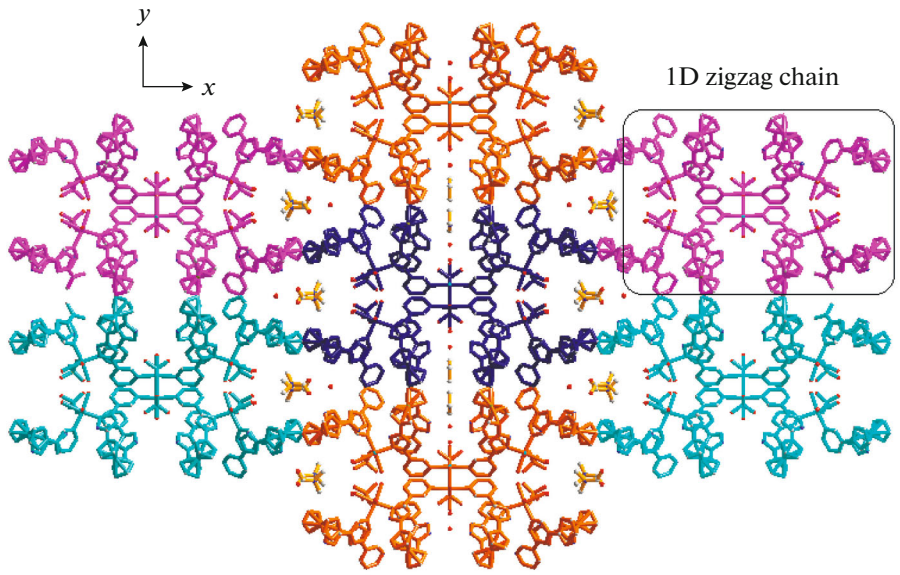

Fig. 5. The 3D supramolecular structure of **II** showing the water molecules occupied the two types of voids.

($E_{1/2}$) of ligands L^1, L^2 and complexes **I**, **II** are shifted towards more positive potentials owing to the substitution of the Cp rings with electron-withdrawing pyrazolyl groups. It is noteworthy that the $E_{1/2}$ of ligands L^1 and L^2 occur at the same potential, suggesting the position of pyridine-N having no effect on the redox behavior of Fc/Fc^+ redox couple. Moreover, as shown in Fig. 7, the CV behavior of complexes **I**, **II** is

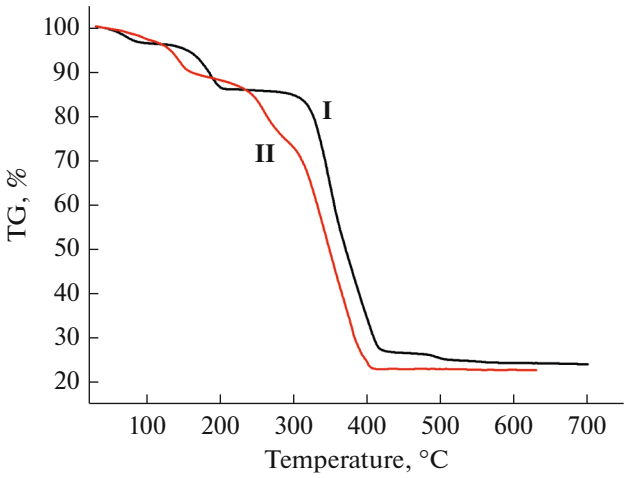

Fig. 6. TG curves for **I** and **II**.

changed comparing with their corresponding ligand. The half-wave potential of **I** is shifted to higher potential than ligand L^1 ($\Delta E_{1/2}$ = 14 mV), showing that the Cd^{2+} can affect the potential of the Fc/Fc^+ couple. For complex **II**, the CV curves lost the reversibility of the Fc/Fc^+ couple and appeared a broad shoulder at a less positive potential than the reduction wave of L^2. This is probably owning to ion-pairing interactions between the oxidized, positively charged Fc^+ of **II** and trace quantity of free SO_4^{2-} in DMF solution [33].

ACKNOWLEDGMENTS

We gratefully acknowledge the financial support by the National Natural Science Foundation of China (no. 21271157), the Foundation and Research in Cutting-Edge Technologies in the Project of Henan Prov-

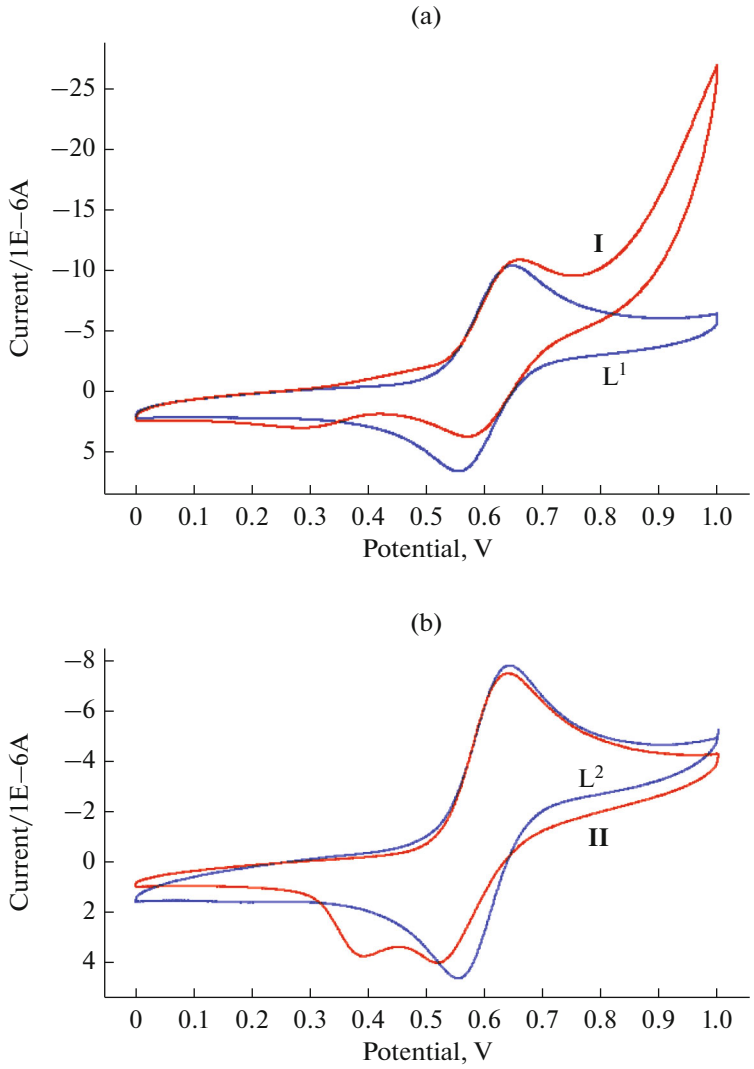

Fig. 7. CVs of L^1 and **I** (a) and L^2 and **II** (b) in DMF. $c_{L1, L2} = 1.0 \times 10^{-3}$ mol L^{-1}; scan rate = 50 mV S^{-1}.

Table 4. Electrochemical parameters of ligands $L^{1, 2}$ and complexes **I**, **II** (~1.0×10^{-3} mol L^{-1})

Compounds	E_{pa}, mV	E_{pc}, mV	ΔE_p, mV	$E_{1/2}$, mV	i_{pa}/i_{pc}
Ferrocene	563	471	92	517	0.917
L^1	643	556	87	600	0.841
L^2	643	556	87	600	0.919
I	659	569	90	614	0.608
II	640	516	124	578	0.634

$\Delta E_p = (E_{pa} - E_{pc})$, $E_{1/2} = (E_{pa} + E_{pc})/2$.

ince (no. 122300410092), and the training and funding Program for young key teacher of Henan University of Urban Construction (G2014009).

REFERENCES

1. Yaghi, O.M., Li, H., Davis, C., et al., *Acc. Chem. Res.*, 1998, vol. 31, p. 474.
2. Eddaoudi, M., Moler, D.B., Li, H., et al., *Acc. Chem. Res.*, 2001, vol. 34, p. 319.
3. Allendorf, M.D., Bauer, C.A., Bhakta, R.K., et al., *Chem. Soc. Rev.*, 2009, vol. 38, p. 1330.
4. Leong, W.L. and Vittal, J.J., *Chem. Rev.*, 2011, vol. 111, p. 688.
5. Rao, C.N.R., Natarajan, S., and Vaidhyanathan, R., *Angew. Chem. Int. Ed.*, 2004, vol. 43, p. 1466.
6. Jainak, C., *Dalton Trans.*, 2003, vol. 17, p. 2781.
7. Wang, X.-L., Liu, P., Lin, H.-Y., et al., *Inorg. Chem. Commun.*, 2013, vol. 30, p. 79.
8. Wang, X.-L., Lin, H.-Y., Mu, B., et al., *Dalton Trans.*, 2010, vol. 39, p. 6187.
9. Cheng, P.-C., Kuo, P.-T., Liao, Y.-H., et al., *Cryst. Growth Des.*, 2013, vol. 13, p. 623.
10. Wang, C.-Y., Wilseck, Z.M., Supkowski, R.M., et al., *CrystEngComm*, 2011, vol. 13, p. 1391.
11. Wilseck, Z.M., Gandolfo, C.M., and La Duca, R.L., *Inorg. Chim. Acta*, 2010, vol. 363, p. 3865.
12. Ma, L.F., Zhao, J.W., Han, M.L., et al., *Dalton Trans.*, 2012, vol. 41, p. 2078.
13. Lo, Y.-C., Hsu, W., He, H.-Y., et al., *CrystEngComm*, 2015, vol. 17, p. 90.
14. Gong, Y.-Q., Chen, J.-T., Yuan, D.-Q., et al., *Inorg. Chim. Acta*, 2007, vol. 360, p. 2207.
15. Zang, S.-Q., Su, Y., Li, Y.-Z., et al., *Inorg. Chem.*, 2006, vol. 45, p. 2972.
16. Togni, A. and Hayashi, T., *Ferrocenes, Homogeneous Catalysis, Organic Synthesis and Materials Science*, Weinheim: VCH, 1995.
17. Li, Z.-F., Li, J.-B., Li, G., et al., *Inorg. Chim. Acta*, 2009, vol. 362, p. 3104.
18. Li, X., Liu, W., Zhang, H.-Y., et al., *J. Organomet. Chem.*, 2008, vol. 693, p. 3295.
19. Meng, X.-R., Hou, H.-W., Li, G., et al., *J. Organomet. Chem.*, 2004, vol. 689, p. 1218.
20. Yang, Y.-Y. and Wong, W.-T., *Chem. Commun.*, 2002, vol. 22, p. 2716.
21. Guo, D., Zhang, B.-G., Duan, C.-Y., et al., *Dalton Trans.*, 2003, vol. 23, p. 282.
22. Cao, C.-Y., Wei, K.-J., Ni, J., et al., *Inorg. Chem. Commun.*, 2010, vol. 13, p. 19.
23. Li, G., Song, Y.-L., Hou, H.-W., et al., *Inorg. Chem.*, 2003, vol. 42, p. 913.
24. Wei, K.-J., Ni, J., Xie, Y.-S., et al., *Dalton Trans.*, 2007, vol. 31, p. 3390.
25. Quintal, S., Fedi, S., Barbetti, J., et al., *J. Organomet. Chem.*, 2011, vol. 696, p. 2142.
26. Aguado, J.E., Calhorda, M.J., Costa, P.J., et al., *Eur. J. Inorg. Chem.*, 2004, vol. 15, p. 3038.
27. Liu, W., Li, X., Zhao, J.-A., et al., *J. Chem. Res.*, 2012, vol. 10, p. 606.
28. Sheldrick, G.M., *SHELX-97, Program for Crystal Structure Analysis: Crystal Structure Dtermination*, Göttingen: Univ. of Göttingen, 1997.
29. Sheldrick, G.M., *SHELX-97, Program for Crystal Structure Analysis: Structure Refinement,* Göttingen: Univ. of Göttingen, 1997.
30. Hu, J.-Y., Liao, C.-L., Zhang, C.-C., et al., *Russ. J. Coord. Chem.*, 2016, vol. 42, p. 378.
31. Wu, W.-P., Liao, Y., Lu, L., et al., *Russ. J. Coord. Chem.*, 2016, vol. 42, p. 355.
32. Li, X., Liu, W., Zhang, H.-Y., et al., *J. Organomet. Chem.*, 2008, vol. 693, p. 3295.
33. Reynes, O., Maillard, F., Moutet, J.C., et al., *J. Organomet. Chem.*, 2001, vol. 637–639, p. 356.